of cytochrome c(III) by hemin Fe(II). A conformational change (k = 17 s^{-1}, 28 °C) was reported.[22] It was also observed that the oxidation of ferrocytochrome c did not result in the same reversible conformational change. As a result of such observations, one should question whether the unimolecular rate observed in this Ru(II)-cyt c(III) intermediate refers directly to the intramolecular electron-transfer process or to different rate-limiting processes as in eq 9a and 9b. In this case the rate-determining step is a

$$\text{Ru(II)-cyt } c\text{(III)} \xrightarrow{k_u} \text{Ru(II)-cyt } c\text{(III)}^* \qquad (9a)$$

$$\text{Ru(II)-cyt } c\text{(III)}^* \rightarrow \text{Ru(III)-cyt } c\text{(II)} \qquad (9b)$$

conformational change and not the electron-transfer process. The interesting point in the observations reported here is the similarity between the intramolecular electron-transfer rate constant (53 s^{-1}) and the unimolecular rate constants reported for these other processes (k = 15-60 s^{-1}). We are currently devising experiments to answer this question. The sensitivity of the rate of electron transfer to driving force will show if the intramolecular electron-transfer step is rate limiting. This can be studied by changing the ligand environment around either the heme site or the ruthenium site. These experiments will be the subject of a future report.

Acknowledgment. The authors thank Dr. Harold Schwarz for his valuable assistance in the pulse radiolysis work and Dr. Carol Creutz, Dr. Norman Sutin, Dr. Michael Simic, and Prof. Henry Taube for helpful discussions. The authors also thank Prof. R. Matthews for providing us a preprint prior to publication and Prof. H. B. Gray for his comments and suggestions on this manuscript. Work done by Rutgers University was supported by the National Institutes of Health Grant GM 26324. S.I. is the recipient of a National Institutes of Health Career Development Award (AM 00734) (1980-85) and a Camille and Henry Dreyfus Teacher Scholar Award (1981-85). Work done at Brookhaven National Laboratories is supported by the Office of Basic Energy Science of the Department of Energy.

Registry No. $CO_2^{\cdot-}$, 14485-07-5; $(CH_3)_2COH^{\cdot}$, 5131-95-3; $(CH_2OH)_3\dot{C}CHOH$, 54954-29-9; $^-O_2CCH(OH)\dot{C}(OH)CO_2^-$, 64672-61-3.

(23) T. Takano, C. Kallai, R. Swanson, and R. E. Dickerson, *J. Biol. Chem.*, **248**, 5234-55 (1973).
(24) N. Sutin, *Acc. Chem. Res.*, **15**, 275-82 (1982).

Electron Transfer across Polypeptides. 2. Amino Acids and Flexible Dipeptide Bridging Ligands[1]

Stephan S. Isied* and Asbed Vassilian

Contribution from the Department of Chemistry, Rutgers, The State University of New Jersey, New Brunswick, New Jersey 08903. *Received June 30, 1983*

Abstract: A series of cobalt(III)-L-ruthenium(III) complexes (I-VIII) with bridging amino acid and dipeptides derivatized with an isonicotinoyl (iso) group at the N-terminal has been synthesized, $[SO_4(NH_3)_4Ru\text{-}(iso\text{-}(AA)_n)\text{-}Co(NH_3)_5]^{3+}$ (I-VIII; n = 0, 1, 2), where for n = 1, AA = Gly, Phe, and Pro and for n = 2, $(AA)_2$ =GlyGly, GlyPhe, GlyLeu, and PhePhe. The effect of these flexible bridging groups on the rate of intramolecular electron transfer and its temperature dependence have been studied. The intramolecular electron-transfer rates for the Gly, Pro, and Phe amino acid complexes were compared with that of the parent isonicotinic acid complex. The unimolecular rate constant (25 °C, 1 M HTFA), $\Delta H^{\ddagger}$, and $\Delta S^{\ddagger}$ for the intramolecular electron transfer from the Ru(II) site to the Co(III) site for the Gly, Pro, and Phe amino acid complexes are 3.8×10^{-5} s^{-1}, 19.9 kcal/mol, -12 eu; 9.9×10^{-5} s^{-1}, 18.0 kcal/mol, -16 eu; and 3.9×10^{-5} s^{-1}, 19.4 kcal/mol, -14 eu, respectively. For the GlyPhe, GlyLeu, GlyGly, and PhePhe dipeptide complexes, the corresponding unimolecular rate constants, $\Delta H^{\ddagger}$ and $\Delta S^{\ddagger}$, are 8.6×10^{-6} s^{-1}, 20.3 kcal/mol, -13.5 eu; 15×10^{-6} s^{-1}, 14.6 kcal/mol, -31.5 eu; 9.9×10^{-6} s^{-1}, 13.3 kcal/mol, -37 eu; and 11.6×10^{-6} s^{-1}, 11.2 kcal/mol, -44 eu, respectively. For the amino acid cases the rates were insensitive to the amino acid side chain. In the dipeptide cases the rate constants are very similar, but the differences between the four flexible dipeptides studied were reflected in the temperature dependence of the rate constant. These differences in the activation parameters are related to the differences in the peptide conformation and hydration properties. The slowness of electron transfer in this series of complexes is attributed to the high reorganizational energy around the cobalt site and to the unfavorable driving force. The reactions, however, go to completion because of the rapid release (ca. $t_{1/2}$ < microseconds) of the ligands from the Co(II) site.

Electron transfer in biological systems takes place through the mediation of a number of proteins, which contain a variety of active sites. The active sites (heme, Fe-S, Cu, and flavin) are generally protected from the solvent, to varying degrees, by a hydrophobic environment created by the polypeptide chain. Recent crystal structures of these electron-transfer proteins[2] have stimulated many speculations concerning the role that the polypeptide chain plays in the electron mediation process. Considerable evidence indicates that rapid electron transfer occurs over long distances (ca. ≥10 Å) between these proteins and their biological partners.[3] However, little is known about the variety of pathways by which peptides participate in the electron-transfer process.

The peptide structure can play a number of roles in the electron-transfer process.[3] One role can be simply *structural*, where the polypeptide chain and the rest of the secondary structure can adjust distances between the sites undergoing electron transfer. Another role that the peptide chain can play is as a *recognition factor*, where a segment of a polypeptide chain, e.g., with positively charged amino acids, helps orient the protein toward a segment of another protein, e.g., with negatively charged amino acids.[4] The *electronic structure of the polypeptide backbone*[5] can be important

(1) A preliminary account of this work has appeared: Isied, S. S. In "Mechanistic Aspects of Inorganic Reactions"; Rorabacher, D., Endicott, J., Eds.; American Chemical Society: Washington, DC, 1982; ACS Symp. Ser. No. 198, p 213.
(2) Adman, E. T. *Biochim. Biophys. Acta* **1979**, *549*, 107-144.
(3) Chance, B., et al., Eds. "Tunneling in Biological Systems"; Academic Press: New York, 1979.
(4) (a) Poulos, T. L.; Kraut, J. *J. Biol. Chem.* **1980**, *255*, 10322-10330. (b) Poulos, T. L.; Kraut, J. *Ibid.* **1980**, *255*, 8199-8205.

0002-7863/84/1506-1726$01.50/0

Table I. Elemental Analyses of Co-(X-iso)-Ru Binuclear Complexes[a]

compd		%C	%H	%N	%Co	%Ru
$[(NH_3)_5Co(Gly\text{-}iso)Ru(NH_3)_4SO_4](BF_4)_3\cdot HBF_4\cdot H_2O$	calcd	10.06	3.91	16.24	6.17	10.59
	obsd	10.26	3.99	15.29	6.24	10.69
$[(NH_3)_5Co(Pro\text{-}iso)Ru(NH_3)_4SO_4](BF_4)_3\cdot HBF_4\cdot H_2O$	calcd	13.29	4.15	15.49	5.92	10.16
	obsd	12.91	4.02	14.41	6.00	10.30
$[(NH_3)_5Co(Phe\text{-}iso)Ru(NH_3)_4SO_4](BF_4)_3\cdot HBF_4\cdot H_2O$	calcd	17.08	4.11	14.61	5.59	9.58
	obsd	17.29	4.31	13.86	5.70	10.10
$[(NH_3)_5Co(Gly\text{-}iso)Ru(NH_3)_4SO_4](BF_4)_3\cdot HBF_4\cdot H_2O$	calcd	11.87	3.99	16.61	5.82	9.99
	obsd	11.20	3.98	15.69	5.40	11.03
$[(NH_3)_5Co(PhePhe\text{-}iso)Ru(NH_3)_4SO_4](BF_4)_3\cdot HBF_4\cdot 3H_2O$	calcd	23.47	4.6	13.69	4.8	8.23
	obsd	23.23	4.35	13.75	4.5	8.0
$[(NH_3)_5Co(GlyPhe\text{-}iso)Ru(NH_3)_4SO_4](BF_4)_3\cdot HBF_4\cdot H_2O$	calcd	18.52	4.21	15.25	5.35	9.17
	obsd	19.17	4.38	15.00	5.50	9.80
$[(NH_3)_5Co(GlyLeu\text{-}iso)Ru(NH_3)_4SO_4](BF_4)_3\cdot HBF_4\cdot H_2O$	calcd	15.75	4.63	15.74	5.52	9.46
	obsd	15.45	4.53	15.68	4.61	9.8

[a] In each of these binuclear complexes the SO_4 is trans to Ru.

in its electron mediation, as seen in the two different forms of the polypeptide.

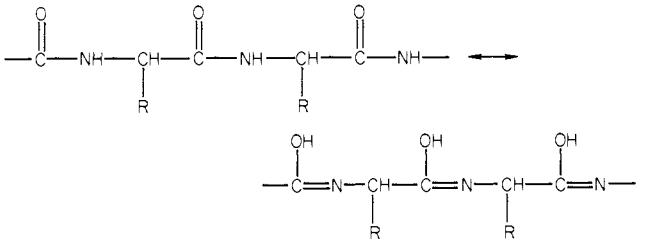

Nonbonding n and π orbitals, as well as empty π^* orbitals of the peptide linkage, may provide electron-transfer pathways.[6-8] *Specific amino acid side chains* such as those of Trp, Phe, and Tyr, as well as sulfur-containing side chains (-SR, -SH, and -SS), can mediate electron transfer through low-lying orbitals.[4,9,10] The above suggestions present a number of chemically plausible pathways where electron transfer is facilitated by the polypeptide chain. However, until now, no systematic studies have been conducted to shed light on any of these pathways.

We have begun a systematic effort to study the effects that amino acids and peptide bridging ligands have when covalently bound to an electron donor and electron acceptor.[1,11] We have synthesized a series of compounds where the peptide bridging group is the only variable. The intramolecular electron-transfer reactions across these polypeptides can now be studied as a single elementary step, uncomplicated by substitution and other processes. The series of complexes that we studied is represented schematically by

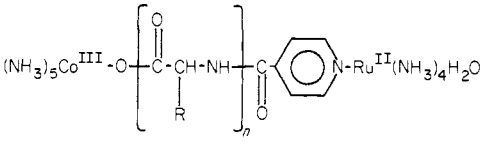

where n = 0, 1, and 2. The oxidizing agent, $(NH_3)_5Co^{III}$-, and the reducing agent, $H_2O(NH_3)_4Ru^{II}$ iso- (where iso = the isonicotinoyl group), are both inert to substitution on the time scale of the electron-transfer experiment. This series of complexes is designed to have the same donor and acceptor metal ions (and thus the same driving force and inner-sphere reorganization energies around the metal ions). The dipeptide bridges include peptides with hydrophobic, hydrophilic, aromatic, aliphatic, and neutral side chains. Although these peptide bridges are flexible (with possible rotation around the α carbon of the amino acids), the difference in the side chains can lead to steric and solvation effects that can bring about differences in rates and activation parameters. In this paper we report on the rates and temperature dependencies of *intra*molecular electron transfer across this series of amino acids and dipeptides.

Scheme I

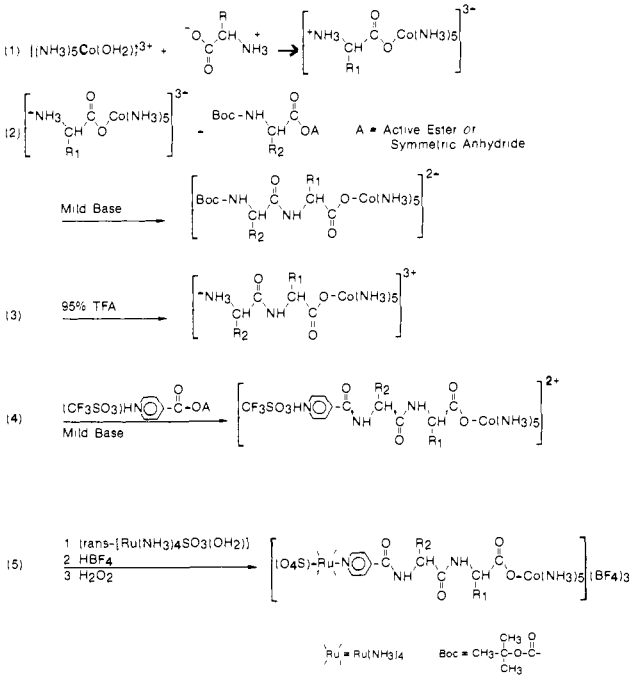

Results

Synthesis of Co(III)-Ru(III) Binuclear Complexes. The stepwise synthesis of the binuclear complexes starting with $[(NH_3)_5Co(OH_2)](ClO_4)_3$ is described in Scheme I. The cobalt(III)-amino acid and -peptide complexes were synthesized by methods described earlier.[12,13] Isonicotinic acid was activated as its trifluoromethanesulfonate salt with dicyclohexylcarbodiimide (DCC) and hydroxybenzotriazole (HOBT) in THF and coupled to the amine end of the different cobalt-amino acid (eq 1 and 5) and -dipeptide (eq 4 and 5) complexes (Scheme I). Intermediates in Scheme I were identified by elemental analysis, by amino acid analysis, and by their retention time on high-pressure liquid

(5) Larsson, S. *J. Am. Chem. Soc.* **1981**, *103*, 4034-4040.
(6) Taube, H. In *Brookhaven Symp. Biol.* **1962**, *No. 15*.
(7) (a) Halpern, J.; Orgel, L. E. *Discuss. Faraday Soc.* **1960**, *29*, 32-41. (b) Halpern, J.; Orgel, L. E. *Ibid.* **1960**, *29*, 7-20.
(8) Evans, M. G.; Gergeley, J. *Biochim. Biophys. Acta* **1949**, *3*, 188.
(9) (a) Williams, R. J. P.; Moore, G. R.; Wright, P. E.; In "Biological Aspects of Inorganic Chemistry"; Addison, A., Cullis, W., Dolphin, D., James B. R., Eds.; Wiley: New York, 1977; pp 369-401. (b) Moore, G. R.; Williams, R. J. P. *Coord. Chem. Rev.* **1976**, *18*, 125.
(10) Hoffman, B. M.; Roberts, J. E.; Brown, T. G.; Kang, C.; Margoliash, E. *Proc. Natl. Acad. Sci. U.S.A.* **1979**, *76*, 6132-6136.
(11) Isied, S. S.; Vassilian, A. *J. Am. Chem. Soc.*, following paper in this issue.
(12) Isied, S.; Vassilian, A.; Lyon, J. *J. Am. Chem. Soc.* **1982**, *104*, 3910.
(13) Isied, S.; Kuehn, C. *J. Am. Chem. Soc.* **1978**, *100*, 6752.

Table II. HPLC Analysis of Cobalt-Peptide and Cobalt-Peptide-Ruthenium Complexes[a]

complex	retention time, min
Co(GlyGly)	2.41
Co(GlyGly-iso)	3.36
Co(GlyGly-iso)Ru	2.31
Co(GlyPhe)	4.05
Co(GlyPhe-iso)	9.45
Co(GlyPhe-iso)Ru	3.68

[a] Solvent system: A, 0.2% TFA in H_2O, pH 2.5; B, 0.2% TFA in MeOH, pH 2.5. Eluent: 30% B, 2 mL/min. $\lambda = 254$ nm. RP C_{18} column (10 μm). Co = $(NH_3)_5Co^{III}$–, Ru = $SO_4(NH_3)_4Ru^{III}$–, iso = isonicotinoyl group.

Table III. Electrochemical Properties of Co-(L-iso)-Ru Binuclear Complexes[a]

complex	$E_{1/2}$, V: Co-(L-iso)-$Ru^{III/II}(NH_3)_4OH_2$	$E_{1/2}$, V: Co-(L-iso)-$Ru^{III/II}(NH_3)_4SO_4$
Co-iso-Ru	0.45	0.33
Co(GlyGly-iso)Ru	0.45	0.33
Co(Gly-iso)Ru	0.45	0.33
Co(ProPro-iso)Ru[b]	0.43	0.33
Co(Pro-iso)Ru	0.44	0.335
Co(PhePhe-iso)Ru	0.45	0.35
Co(Phe-iso)Ru	0.45	0.34
Co(GlyPhe-iso)Ru	0.44	0.35

[a] $E_{1/2}$ determined by differential pulse polarography in 0.1 M HTFA on a Pt-button electrode; V vs. NHE; Co = $(NH_3)_5Co^{III}$–, Ru = $SO_4(NH_3)_4Ru^{III}$–, L = amino acid or peptide; scan rate = 2 mV/s; potentials are ±0.01 V. [b] Reference 11.

chromatography (HPLC)[14] using octadecylsilane-derivatized silica gel columns.

Characterization of the Binuclear Complexes. The elemental analyses of the Co(III)–Ru(III) products are listed in Table I. The retention times of the various synthetic intermediates for two dipeptides on HPLC are listed in Table II. The difference in retention time between the cobalt–amino acid and –peptide complexes with and without the isonicotinoyl group served as a method for monitoring the incorporation of the isonicotinoyl group onto the cobalt–peptide complex and for further purification of the complexes.

The visible absorption spectra of the Co^{III}–(L-iso)–Ru^{III} complexes show bands typical of the Co(III) center ($\lambda \sim 501$ and 350 nm). The latter band appears as a shoulder and is sometimes masked by strong UV absorption of the Ru(III) heterocycle. Reduction of these complexes to Co^{III}–(L-iso)–Ru^{II} complexes with $[(NH_3)_6Ru]^{2+}$ or Eu^{2+} produces the intense absorption band characteristic of the Ru(II) metal-to-ligand charge-transfer band. For all the amino acids and dipeptides the λ_{max} is 478 nm ($\epsilon \sim 1 \times 10^4$ M^{-1} cm^{-1}), except for the proline derivative, where λ_{max} is 458 nm ($\epsilon \sim 0.8 \times 10^4$ M^{-1} cm^{-1}). The parent compound Ru^{II}–iso–Co^{III} (I) has $\lambda_{max} = 490$ nm ($\epsilon \sim 1.1 \times 10^4$ M^{-1} cm^{-1}).

The electrochemical properties of the binuclear complexes were investigated by using differential pulse polarography (see Experimental Section). When the Co^{III}–(L-iso)–Ru^{III} complexes were reduced electrochemically, two reduction waves were observed (Table III). These were assigned to the $[SO_4(NH_3)_4Ru^{III/II}$–(iso-L)–Co] and $[H_2O(NH_3)_4Ru^{III/II}$–(iso-L)–Co couples[15] (where Co = $(NH_3)_5Co$). When the Co^{III}–(L-iso)–Ru^{III} complexes were reduced with Eu^{2+} to generate the $[H_2O(NH_3)_4Ru^{II}$–(iso-L)–$Co^{III}]$ species first and then oxidized electrochemically, only the one wave corresponding to the $[H_2O(NH_3)_4Ru^{III/II}$–(iso-L)–Co] couple was observed.

Intramolecular Rates of Electron Transfer. The rate of intramolecular electron transfer was determined by monitoring the decrease in absorbance at 480 nm (Ru(II)–pyridine charge transfer). This corresponds to the oxidation of Ru(II) to Ru(III). The rate of intramolecular electron transfer follows the equation

$$\text{rate} = k[Ru^{II}\text{–bridge–}Co^{III}] \quad (6)$$

The Ru^{II}–bridge–Co^{III} precursor complexes were generated in solution from the Ru^{III}–bridge–Co^{III} complexes by using either $[(NH_3)_6Ru]^{2+}$ or Eu^{2+}. In both cases similar rates were obtained. The first-order dependence of the rate constant was established by varying the Ru^{II}–bridge–Co^{III} concentration by a factor of greater than 4. The Ru^{III}–bridge–Co^{III} was also varied by a factor of 2 (Table IV). Experiments were done at low concentrations of precursor complex (ca. $<10^{-4}$ M) in order to avoid interference by intermolecular reactions. Table IV shows the rate constants at various concentrations of Ru^{III}–bridge–Co^{III} and Ru^{II}–bridge–Co^{III} using $[Ru(NH_3)_6]^{2+}$. The redistribution of Ru(II) between the precursor complex and the mononuclear species formed during the progress of the reaction is minimized by using an excess of the Co^{III}–bridge–Ru^{III} binuclear complex. Table V shows the variation of rate at different temperatures for the complexes studied. Tables VI and VII summarize the rate and activation parameters obtained for the amino acid and peptide bridging ligands, respectively. The structure of the bridging group is shown to facilitate the comparison.

In a number of experiments Eu^{2+} was used as a reductant instead of $[Ru(NH_3)_6]^{2+}$. Results from these experiments showed identical rates of intramolecular electron transfer within experimental error. For example, for $[Co^{III}(Gly\text{-}iso)Ru^{III}] = 7.9 \times 10^{-4}$ M, when reduced with 7.3×10^{-5} M Eu^{2+} in 1 M HTFA, the measured intramolecular rate was 4.05×10^{-5} s^{-1}, which compares well with the $[Ru(NH_3)_6]^{2+}$ results (Table VI).

Results on the effect of Cl^- on the rates of intramolecular electron transfer for some of the amino acids and dipeptides are shown in Table VIII and compared with the results using HTFA. A rate enhancement by Cl^- is observed.

Table IV. Intramolecular Electron-Transfer Rates at Various Complex Concentrations[a]

(complex), M	$([NH_3)_6Ru]^{2+}$), M	temp, °C	10^5k, s^{-1}
	Co^{III}(Pro-iso)Ru^{III}		
8.0×10^{-4}	5.7×10^{-5}	24.8	11.0
1.26×10^{-3}	11.5×10^{-5}	25.5	12.5
1.5×10^{-3}	11.5×10^{-5}	25.5	11.4
	Co^{III}(GlyPhe-iso)Ru^{III}		
9.1×10^{-4}	5.7×10^{-5}	24.8	0.89
9.1×10^{-4}	11.5×10^{-5}	25.5	1.01
	Co^{III}(Gly-iso)Ru^{III}		
7.9×10^{-4}	5.7×10^{-5}	24.8	3.90
7.9×10^{-4}	1.8×10^{-4}	24.8	3.57

[a] 1.0 M HTFA.

Table V. Electron-Transfer Rate Constants at Different Temperatures

complex[b]	10^5k,[a] s^{-1}: 24.8 °C	29.0 °C	33.2 °C	37.7 °C
Co(Gly-iso)Ru (II)	3.84	6.5	9.9	16.5
Co(pro-iso)Ru (III)	10.4	18.7	27.8	38.6
Co(Phe-iso)Ru (IV)	3.87	6.4	9.3	15.8
Co(GlyGly-iso)Ru (VII)	1.04	1.45	1.7	2.87
Co(GlyPhe-iso)Ru (V)	0.87	1.37	2.4	3.68

complex	10^5k,[a] s^{-1}: 24.7 °C	29.5 °C	33.6 °C	39.0 °C
Co(GlyLeu-iso)Ru (VI)	1.50	2.81	3.6	5.2
Co(PhePhe-iso)Ru (VIII)	1.2	1.4	1.6	2.35

[a] Each rate constant is the average of two different determinations. [b] Co = $(NH_3)_5Co$–, Ru = $(OH_2)(NH_3)_4Ru$–; see Tables VI and VII for structures of the complexes. $[Co^{III}(bridge\text{-}iso)Ru^{III}] = 1 \times 10^{-3}$–$5 \times 10^{-4}$ M and $[Co^{III}(bridge\text{-}iso)Ru^{II}] = 5.7 \times 10^{-5}$–$5.9 \times 10^{-5}$ M in 1.0 M HTFA, where bridge = amino acid or peptide.

(14) Isied, S.; Lyon, J.; Vassilian, A. *J. Liq. Chromatogr.* **1982**, *5*, 537–547.
(15) Isied, S.; Taube, H. *J. Am. Chem. Soc.* **1973**, *95*, 8198.

Table VI. Intramolecular Electron-Transfer Rates and Activation Parameters across Amino Acids[a]

complex	bridge	k(25 °C), s^{-1}	$\Delta H^{\ddagger}$, kcal/mol	$\Delta S^{\ddagger}$, eu
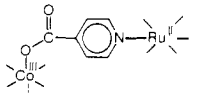 I	iso	1.24×10^{-2}	19.7 ± 0.2	−1.0 ± 0.5
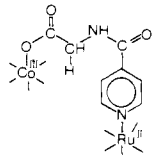 II	Gly-iso	3.8×10^{-5}	19.9 ± 0.3	−12 ± 1
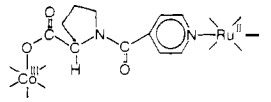 III	Pro-iso	10.4×10^{-5}	18.0 ± 1.1	−16 ± 4
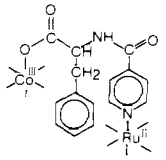 IV	Phe-iso	3.9×10^{-5}	19.4 ± 0.8	−14 ± 3

[a] Medium: 1 M HTFA.

Intermolecular Reactions. In order to evaluate the possible interference from intermolecular reactions the rate of the following model reaction was studied.

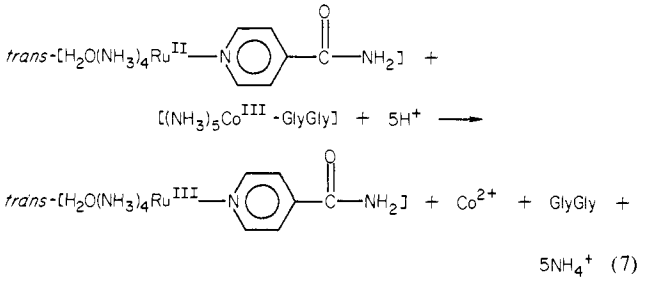

The rate of this reaction followed second-order kinetics

$$\text{rate} = k_b[Ru^{II}][Co^{III}\text{-peptide}] \quad (8)$$

with $k_b = 2.4 \times 10^{-3}$ M^{-1} s^{-1} at 25.0 °C and 0.1 M HTFA.

Discussion

In this paper we have studied a series of *intra*molecular electron-transfer reactions in order to obtain information on the properties of the bridging amino acid and peptide ligand. For the type of complexes studied here the intermolecular reaction follows second-order kinetics, while the intramolecular reaction follows first-order kinetics. At low concentrations (ca. 5×10^{-5} M precursor complex), these intramolecular reactions can be studied without interference from the intermolecular reaction. In order to verify this, we have measured the *inter*molecular rate of electron transfer for eq 7 (as a model for the intermolecular reaction). In this reaction the cobalt and ruthenium moieties are separate molecules, each containing part of the bridging ligand. The rate constant observed, $k = 2.4 \times 10^{-3}$ M^{-1} s^{-1} (25 °C, 1 M HFTA), implies that interference from intermolecular reactions is negligible (<5%) at the concentration of precursor complex studied (ca. 5×10^{-5} M).

The amino acid and dipeptide bridging complexes studied have similar redox potentials (Table III) and similar inner-sphere reorganization energies, because the coordination environment around the Ru and Co centers is kept constant. With these parameters held constant, a detailed examination of the electron-transfer properties of the amino acid and peptide bridging ligands becomes possible. Addition of the first amino acid residue, i.e., Gly (II), Phe (IV), and Pro (III), to the isonicotinic acid complex (Table V) results in a decrease in the rate of approximately 100–500 for the three different amino acids used. No significant difference was observed among the flexible amino acids, Gly (II) and Phe (IV), and the rigid amino acid, Pro (III). The rate of intramolecular electron transfer across Phe (IV) (where a benzyl group replaces a hydrogen atom as the side chain) is not much different from that across Gly (II). The rate constant for the Pro (III) is about 3 times greater than that for the Gly (II) or Phe (IV). This difference may be explained by the rigidity of the proline linkage, which helps keep the metals apart at a fixed distance. The difference in rate between parent compound I and compounds II–IV, when one amino acid is placed between the cobalt and ruthenium sites, is reflected mainly in the activation entropy, $\Delta S^{\ddagger}$ (the $\Delta H^{\ddagger}$ values for these compounds are the same within experimental error).

For the flexible dipeptides (Table VII), the rate of intramolecular electron transfer decreases slightly from that for the amino acids. The rate constant for the dipeptides among the series is constant to within a factor of 2. This at first glance indicates that electron transfer in these binuclear complexes is not sensitive to the nature of the dipeptide. However, when the activation parameters for the flexible dipeptides studied are examined, significant differences are observed. There is a variation of $\Delta H^{\ddagger}$ between 20 and 11 kcal/mol and a decrease of $\Delta S^{\ddagger}$ from −13 to −44 eu. Because the donor and acceptor metal ions are kept constant, the variation in rate and activation parameters can be related to the structure, conformation (distance between the metal centers), and hydration properties of the bridging amino acids and peptides. The variation in activation parameters within the series of complexes can be accounted for by considering three parameters: (a) outer-sphere reorganization energy, $\Delta G^{\ddagger}_{out}$, (b) electronic coupling, H_{AB}, and (c) the work required to bring the two ends of the molecule together, $\Delta G^{\ddagger}_{w}$. These three parameters depend on the distance between the two metal ions in the transition state.

The outer-sphere reorganization energy depends on distance according to the Hush–Marcus model[16a]

$$\Delta G^{\ddagger}_{out} = \frac{(\Delta q)^2}{4}\left\{\frac{1}{2a_1} + \frac{1}{2a_2} - \frac{1}{d}\right\}\left\{\frac{1}{n^2} - \frac{1}{D_s}\right\} \quad (9)$$

Table VII. Intramolecular Electron-Transfer Rates and Activation Parameters across Dipeptides[a]

complex	bridge	k(25 °C), s^{-1}	$\Delta H^{\ddagger}$, kcal/mol	$\Delta S^{\ddagger}$, eu
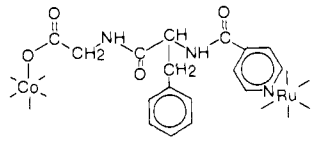 V	GlyPhe-iso	8.6×10^{-6}	20.3 ± 0.9	−13.5 ± 3
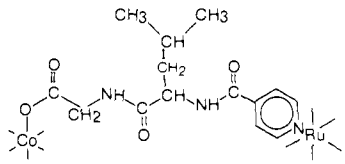 VI	GlyLeu-iso	15×10^{-6}	14.6 ± 1	−31.5 ± 3
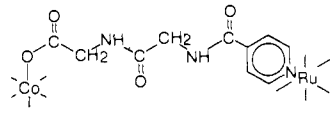 VII	GlyGly-iso	9.9×10^{-6}	13.3 ± 1.2	−37 ± 4
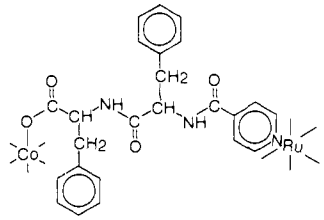 VIII	PhePhe-iso	11.6×10^{-6}	11.2 ± 1.0	−44 ± 3

[a] Medium: 1 M HTFA.

Table VIII. Effect of Cl$^-$ on the Rate of Intramolecular Electron Transfer

complex	10^5k, s^{-1} chloride[a]	trifluoroacetate[b]
Co(Gly-iso)Ru (II)	25	3.8
Co(Phe-iso)Ru (IV)	17.4	3.9
Co(GlyGly-iso)Ru (VII)	10	1.04
Co(GlyPhe-iso)Ru (V)	15.6	0.87
Co(ProPro-iso)Ru[c]	7.4	0.64

[a] 1.0 M HCl, 25 °C. [b] 1.0 M HTFA, 25 °C. [c] Reference 11. Co = $(NH_3)_5Co^{III}$–; Ru = $(OH_2)(NH_3)_4Ru^{II}$–.

where a_1 and a_2 are the radii of the two reactants, Δq is the difference in net charge of the two reactants, n is the refractive index, D_s is the static dielectric constant, and d is the distance between the centers of the two reactants in the activated complex. In this work eq 9 reduces to $\Delta G^{\ddagger}_{out} = (12.85 - 45/d)$ kcal mol^{-1} for $a_1 = a_2 = 3.5$ Å. At zero ionic strength $\Delta G^{\ddagger}_{out} \approx \Delta H^{\ddagger}_{out}$,[16c] and the contribution of $\Delta H^{\ddagger}_{out}$ to the activation barrier for electron transfer is calculated to be between 1.5 and 2.5 kcal mol^{-1}, increasing with an increase in distance between the metal centers in the transition state.

The electronic coupling element, H_{AB}, decreases as the distance between the two metal ions increases. Using a modified form of Hopfield's equation,[16b] one can approximate the electronic coupling element, H_{AB}, as[16a]

$$H_{AB} = H^{\circ}_{AB} e^{-\alpha(d-\sigma)} \tag{10}$$

where d is the metal-to-metal distance, $\sigma = a_1 + a_2$ (sum of the radii of the reactants), α is estimated as 0.72 Å^{-1}, and H°_{AB} equals H_{AB} when $d = \sigma$. The origin of the large decrease in rate upon introduction of the first amino acid is attributed to a decrease in the electronic coupling. This is shown as a decrease in $\Delta S^{\ddagger}$ (Table VI); thus substantial nonadiabaticity is present with the introduction of the bridging ligand.

The work required to bring the Co(III) and Ru(II) metal centers to close proximity also affects the activation parameters for the electron-transfer reaction. The electrostatic energy between these two positively charged ions can be expressed as

$$\Delta G^{\ddagger}_{w} = Z_1 Z_2 / D_s r \tag{11}$$

where D_s is the dielectric constant, r is the metal-to-metal distance, and Z_1 and Z_2 are +2 and +3, the charges on Ru(II) and Co(III). The associated $\Delta S^{\ddagger}_{w}$ and $\Delta H^{\ddagger}_{w}$ can be expressed as

$$\Delta S^{\ddagger}_{w} = \frac{\Delta G^{\ddagger}_{w}}{T}\left\{\frac{\partial \ln D_s}{\partial \ln T}\right\} \tag{12}$$

$$\Delta H^{\ddagger}_{w} = \Delta G^{\ddagger}_{w}\left\{1 + \frac{\partial \ln D_s}{\partial \ln T}\right\} \tag{13}$$

The $\Delta G^{\ddagger}_{w}$ is positive for bringing a +2 charge close to a +3 charge, while $\Delta S^{\ddagger}_{w}$ is negative because D_s decreases with increasing temperature. The derivative $\partial \ln D_s/\partial \ln T = -1.368$ in water at 25 °C. Therefore eq 12 and 13 reduce to $\Delta S^{\ddagger}_{w} = -1.368 \cdot \Delta G^{\ddagger}_{w}/T$ and $\Delta H^{\ddagger}_{w} = -0.368(\Delta G^{\ddagger}_{w})$. Since $\Delta G^{\ddagger}_{w}$ is positive, both $\Delta S^{\ddagger}_{w}$ and $\Delta H^{\ddagger}_{w}$ are negative. This means that when the oxidant and reductant are in close proximity in the transition state, a lowering of $\Delta H^{\ddagger}$ is expected. This is also accompanied by a more negative $\Delta S^{\ddagger}$. Thus, for the series of flexible dipeptides studied, the distance between the Co and Ru centers is the factor that modulates the $\Delta H^{\ddagger}$ and $\Delta S^{\ddagger}$ parameters. The $\Delta H^{\ddagger}$ is expected to increase with increasing distance (outer-sphere reorganization energy, eq 9) and will decrease if the donor and acceptor come into close proximity (eq 13). The $\Delta S^{\ddagger}$ will decrease when the donor and acceptor are in close proximity (eq 12) and will also decrease with increasing distance (electronic coupling). This analysis assumes no variation in ΔS°, the thermodynamic entropy

(16) (a) Sutin, N. *Acc. Chem. Res.* **1982**, *15*, 275–282. (b) Hopfield, J. In "Tunneling in Biological Systems"; Chance, B., et al., Eds.; Academic Press: New York, 1979. (c) Sutin, N. In ref 16b.

of the electron-transfer reaction, throughout the series; otherwise a correction must be made for each case.

The distance between the two redox centers in the complexes studied can vary over only a small range (i.e., the distance between the two ions cannot be larger than the extended dipeptide structure). The metal–metal distance in these dipeptides can be as far apart as 15 Å or as close as 7 Å, as calculated from space-filling molecular models. It is within this 8-Å range that the various dipeptides assume different average distances. Such properties result in the varied activation parameters observed in Table VII.

In the next paper[11] we show that for a rigid dipeptide with two prolines separating the metal centers, a large $\Delta H^{\ddagger}$ (18.6 kcal/mol) and a negative $\Delta S^{\ddagger}$ (−20 eu) are observed. In this rigid molecule the donor and acceptor cannot come to as close a proximity as in the other flexible molecules. One therefore expects no decrease in $\Delta H^{\ddagger}$ or in $\Delta S^{\ddagger}$, as a result of the work required to bring the positive metal centers together, since these activation parameters refer to the extended form of this rigid dipeptide. For the other flexible dipeptides in this series, the lower the $\Delta H^{\ddagger}$, the shorter is the average distance between the metal centers in the activated complex.

In this study the intramolecular electron-transfer reactions are very slow ($t_{1/2} \sim$ many hours). Even when there is no peptide separating the cobalt and ruthenium centers, a slow rate of electron transfer ($t_{1/2} \sim$ minutes) is observed. There are two main factors that decrease the rate of electron transfer in these binuclear complexes: (a) the reorganization energies around the cobalt and ruthenium centers, with the cobalt center providing the major barrier, and (b) the driving force for the reaction, which is the difference in the $E_{1/2}$ for the $Ru^{II/III}$ and the $Co^{II/III}$ couples. The $E_{1/2}$ for the $Ru^{II/III}$ site in these complexes has been measured (Table III). However, no values for the cobalt site are available. We estimated the potential of the $Co^{II/III}$ site using the recent self-exchange rate of $[Co(NH_3)_6]^{3/2+}$ [17] and the Marcus relation as $E_{1/2} \sim -0.1$ V vs. NHE. This leads to the conclusion that the driving force for the intramolecular electron-transfer reaction we have studied is +0.5 V (11.5 kcal/mol; i.e., the reaction is endothermic). This endothermicity results in a decrease of the rate by several orders of magnitude. The reaction however goes to completion, in spite of this endothermicity, because the Co^{II} center loses its ligands very rapidly (submicrosecond time scale) and this drives the reaction to completion.

As mentioned in the Results, some of the electron-transfer reactions were studied by using HCl, as well as HTFA media. The $[H_2O(NH_3)_4Ru^{II}-]$ is known to undergo substitution in high-Cl^- media to form the $[Cl(NH_3)_4Ru-]$[18] ($K_{eq} \sim 1$). The chloro complex is more reducing than the aquo analogue by approximately 150 mV. This increase in driving force is expected to speed up the reaction by approximately a factor of 10, as observed (Table VIII).[19]

In summary, the introduction of an amino acid between the two metal complexes decreases the rate of intramolecular electron transfer by 2 orders of magnitude, and this is reflected mainly in the negative entropy of activation. For the flexible dipeptides, the rates of the intramolecular electron transfer remain constant, but large variation in the temperature dependence of the rate is observed for different dipeptide bridging groups. The peptide conformation and hydration properties are the only variables to account for the variation in the temperature dependence of the rate constant.

In this study we have not obtained any proof for the possible mechanisms of electron transfer involving amino acids and peptides discussed in the introduction. We have however defined an approach that can be extended to more sophisticated models where the time scale of electron transfer can be varied by controlling the properties of the donor and acceptor pair. It is expected that at faster electron-transfer time scales, these peptides will have to discriminate between the different mechanisms available to them. We are currently extending this work to donors and acceptors that are known to undergo electron transfer at much faster time scales.

Experimental Section

Chemicals. L-Amino acids (99.9% pure) were purchased from Aldrich Chemical Co. and Tridom Chemical Co. Boc-amino acids were purchased from Bachem (Torrance, CA) and Peninsula Labs (San Carlos, CA). Solvents, including DMF, CH_2Cl_2, THF, and ethyl acetate (EtAc), were all glass-distilled and kept dry with molecular sieves. Other solvents (ethanol and ether) were reagent grade and were used as supplied. Trifluoroacetic acid (TFA) was purchased from Aldrich and Fisher Scientific. Dicyclohexylcarbodiimide (DCC) and hydroxybenzotriazole (HOBT) were purchased from Pierce Chemical Co. and Tridom Chemical Co. Trifluoromethanesulfonic acid was purchased from 3M Co.

Resins, Packings, and HPLC Solvents. Pre-Pak 500-C_{18} packing (37–50 μ) (Waters) was used for preparative reverse-phase chromatography. Bio-Gel P-2 (200–400 mesh) and Chelex 100 (100–200 mesh) ion exchange resins were purchased from Bio-Rad Labs. HPLC-grade methanol was purchased from JT Baker Co. HPLC solvents were filtered through Millipore membranes (Millipore Corp.).

I. Pentaamminecobalt–Amino Acid and –Peptide Complexes. The pentaamminecobalt–amino acid and –dipeptide complexes were synthesized by the method of Isied et al.[11]

II. Preparation of Isonicotinic Acid Trifluoromethanesulfonate (A). To 4.0 g of isonicotinic acid (recrystallized from water), CF_3SO_3H was added dropwise with stirring until the isonicotinic acid dissolved. Then ethanol (~10 mL) was added, followed by ethyl ether until turbidity began to appear. The resulting solution was cooled in ice to complete the precipitation. The solid was filtered, washed with ether, and dried over P_2O_5 in a vacuum desiccator overnight.

III. Preparation of $[(NH_3)_5Co$–X–isonicotinoyl$]^{2+}$, where X = Gly, Pro, Phe, GlyGly, ProPro, GlyPhe, GlyLeu, and PhePhe. To a THF solution (4.0 mL) of A (6.0 mmol, 1.64 g) was added 0.92 g of HOBT (6.0 mmol) in 1.5 mL of DMF, followed by 1.24 g of DCC (6.0 mmol) in 1 mL of CH_2Cl_2. Formation of the active ester of A was left to proceed for 1 h at room temperature, and then the dicyclohexylurea precipitate that formed was filtered off. To the filtrate was added 1.0 mmol of $[(NH_3)_5Co$–X$](BF_4)_3$[11] in 1 mL of DMF, followed by 1 mL (9.1 mmol) of *N*-methylmorpholine. This solution was stirred for 2 h to complete the coupling. The coupling reaction was monitored by following the disappearance of the band corresponding to $[(NH_3)_5Co$–X$]^{3+}$ by HPLC.

After the coupling was complete, the mixture was filtered again, and the filtrate was evaporated to a viscous liquid. Ethyl acetate (~15 mL) was added and the desired compound was extracted with 2% aqueous acetic acid. This acetic acid solution was then applied to an ion exchange column (2 × 15 cm) containing Chelex 100 (200–400 mesh) and washed with 2% HOAc until no isonicotinic acid remained. The compound was then eluted with 1.0 M HTFA, collected, and used directly in the synthesis of the binuclear complexes. In the cases where X = GlyGly and Pro, the cobalt complexes were further characterized as BF_4^- salts. This was done by eluting the cobalt complex with HBF_4 (1 M), instead of HTFA, and further purifying by gel filtration (Bio-gel P-2, 200–400 mesh).

IV. Preparation of Cobalt–X–Iso–Ruthenium Binuclear Complexes. *trans*-$[Ru(NH_3)_4SO_2Cl]Cl$ (0.93 mmol, 0.284 g) was added to an argon-degassed solution of $[(NH_3)_5Co$–X–iso$]^{3+}$ (0.93 mmol) (where X = Gly, Phe, Pro, GlyGly, GlyPhe, ProPro, GlyLeu, and PhePhe and iso = isonicotinoyl group) in 2 mL of water. Solid $NaHCO_3$ was added until the solution was pH 8.3. The solution turned orange-red. The reaction was left for 2 min and then transferred to a flask containing 5 mL of 48% HBF_4. Hydrogen peroxide (30%) was added dropwise with stirring until the orange color disappeared. Ethanol (75 mL) was added. The precipitate that formed was filtered and the solid was washed with ethanol and ether.

The solid was dissolved in 2 mL of 2% aqueous acetic acid, chromatographed on a C_{18}-derivatized silica gel reverse-phase column (25 cm × 2.5 cm), and eluted with 2% acetic acid. The orange band was collected, rotoevaporated to dryness, dissolved in 1.0 mL of 5.0×10^{-4} M HBF_4, applied to a Bio-Gel P-2 column (200–400 mesh) (30 cm × 1 cm),

(17) (a) Gezelowitz, D. Ph.D. Thesis, Stanford University, 1982. (b) The potential of the $Co^{II/III}$ couple was estimated by using the Marcus relationship and data from the reaction

$$[(NH_3)_6Ru^{II}-] + [(NH_3)_5Co^{III}(GlyGly)] \xrightarrow{k = 2 \times 10^{-3}\ M^{-1}\ s^{-1}} \text{product}$$

(Silverman, M.; Isied, S., unpublished work). The self-exchange rates of $[(NH_3)_6Ru]^{2/3+}$ and that of $[(NH_3)_5Co^{II/III}(GlyGly)]$ (as an approximation for $[(NH_3)_6Co]^{2/3+}$) were also used.

(18) Marchant, J. A.; Matsubara, T.; Ford, P. C. *Inorg. Chem.* **1977**, *16*, 2160–2165.

(19) The acid-catalyzed substitution of Cl^- at the Co(III) carboxylate site is a process that can compete with the electron-transfer process. For this reason the majority of our studies were conducted in HTFA media.

and eluted with 5×10^{-4} M HBF_4. The main orange band was collected, rotoevaporated to dryness, and analyzed (see Results).

Methods. HPLC was performed on a Waters Associates liquid chromatography system equipped with a variable-wavelength UV detector and a fixed-wavelength detector, in order to monitor two different wavelengths simultaneously when needed. A solvent system containing water/methanol with up to 0.2% TFA was used for the elution of cobalt complexes of hydrophobic peptides. The progress of each reaction was followed by using Radial Pak C_{18} cartridges (10-μm octadecylsilane columns, 8 mm × 10 cm, Waters) and a Waters Radial Compression (Model RCM 100) or Altex C_{18} columns (5 μm, 4.6 mm × 25 cm) with flow rates of 1-2 mL/min.

Differential pulse measurements were done on the complexes by using a PAR Model 174A polarographic analyzer, and cyclovoltammograms were recorded with a PAR Model 173 potentiostat, a Model 175 universal programmer, and an Omnigraph 2000 X-Y recorder. Detailed electrochemical measurements were done by using differential pulse polarography because of the presence of two overlapping waves. A Pt-button working electrode was used in a three-electrode configuration with SCE as the reference electrode.

Kinetic Experiments. Solutions of the binuclear complexes of 0.5×10^{-3} to 1.5×10^{-3} M were freshly prepared by dissolving the appropriate weight of the complex in 1.8 mL of 1 M HTFA and degassing the resulting solution with argon in a Zwickel flask for 30 min. In a separate flask $[(NH_3)_6Ru]Cl_3$ was dissolved in 0.1 M HTFA and reduced over Zn/Hg, and 0.2 mL of this solution was added to the binuclear complex to generate the desired concentration of the Ru^{II}-L-Co^{III} precursor complex ($\sim 5 \times 10^{-5}$ M). The rate of intramolecular electron transfer was monitored spectrophotometrically at $\lambda = 480$ nm for all the reactions studied. The temperature was controlled by using a thermostated cell compartment. For the fast reactions ($k > 10^{-4}$ s^{-1}), data were collected for the entire reaction. For the slow reactions, data were collected for up to 10% reaction. The reactions were then quenched with a slight excess of ammonium persulfate and the absorbance (A_∞) was measured immediately. The ratio of (Ru^{III}-L-Co^{III})/(Ru^{II}-L-Co^{III}) was always maintained between 10 and 25. This was found to be necessary to prevent interference of the product formed during the reaction.[15]

The intermolecular reactions were also studied in an argon atmosphere. The $[OH_2(NH_3)_4Ru^{II}$-isn) solution (where isn = isonicotinamide), prepared by reducing the corresponding $[SO_4(NH_3)_4Ru^{III}$-isn] with $[(NH_3)_6Ru^{II}]$,[15] was added to the $[(NH_3)_5Co(GlyGly)](BF_4)_3$ to make the final concentration of the ruthenium complex 5×10^{-5} M and the final concentration of $[(NH_3)_5Co(GlyGly)]^{3+}$ 5×10^{-3} M in 1 M HTFA. The decrease in absorbance was monitored at $\lambda = 480$ nm. Pseudo-first-order rate constants k_{obsd} (s^{-1}) and second-order rate constants k_b (M^{-1} s^{-1}) were evaluated from the absorbance vs. time data.

Treatment of Data. Rate constants for the fast reactions ($k > 10^{-4}$ s^{-1}) were obtained from the slopes of the least-squares plots of ln ($A_\infty - A_t$) vs. t. For the slow reactions, the initial rate method was used. $\Delta H^\ddagger$ was calculated from the least-squares fit of ln k/T vs. $1/T$ plots. The $\Delta S^\ddagger$ values were then calculated from the high and low limits of $\Delta H^\ddagger$.

Acknowledgment. This work was supported by the National Institutes of Health (Grant 26324). S.I. is the recipient of a National Institutes of Health Career Development Award (AM 00734) (1980-1985) and a Camille and Henry Dreyfus Teacher-Scholar Award (1982-1986). S.I. gratefully acknowledges helpful discussions with Professor H. Taube.

Registry No. $[(NH_3)_5Co(Gly\text{-}iso)Ru(NH_3)_4SO_4](BF_4)_3 \cdot HBF_4$, 88510-33-2; $[(NH_3)_5Co(Pro\text{-}iso)Ru(NH_3)_4SO_4](BF_4)_3 \cdot HBF_4$, 88510-36-5; $[(NH_3)_5Co(Phe\text{-}iso)Ru(NH_3)_4SO_4](BF_4)_3 \cdot HBF_4$, 88510-39-8; $[(NH_3)_5Co(GlyGly\text{-}iso)Ru(NH_3)_4SO_4](BF_4)_3 \cdot HBF_4$, 88496-22-4; $[(NH_3)_5Co(PhePhe\text{-}iso)Ru(NH_3)_4SO_4](BF_4)_3 \cdot HBF_4$, 88496-25-7; $[(NH_3)_5Co(GlyPhe\text{-}iso)Ru(NH_3)_4SO_4](BF_4)_3 \cdot HBF_4$, 88496-28-0; $[(NH_3)_5Co(GlyLeu\text{-}iso)Ru(NH_3)_4SO_4](BF_4)_3 \cdot HBF_4$, 88510-42-3; $[(NH_3)_5Co\text{-}iso\text{-}Ru(NH_3)_4SO_4](BF_4)_3$, 88547-64-2; $[(NH_3)_5Co(GlyGly)](BF_4)_3$, 68582-25-2; $[(NH_3)_5Co(GlyPhe)](BF_4)_3$, 68582-27-4; $[(NH_3)_5Co\text{-}Gly](BF_4)_3$, 68582-21-8; $[(NH_3)_5Co\text{-}Pro](BF_4)_3$, 68582-23-0; $[(NH_3)_5Co\text{-}Phe](BF_4)_3$, 81688-40-6; $[(NH_3)_5Co\text{-}(ProPro)](BF_4)_3$, 68582-29-6; $[(NH_3)_5Co\text{-}(GlyLeu)](BF_4)_3$, 88496-31-5; $[(NH_3)_5Co\text{-}(PhePhe)](BF_4)_3$, 88496-34-8; $[(NH_3)_5Co(GlyGly\text{-}iso)]^{2+}$, 88496-35-9; $[(NH_3)_5Co(GlyPhe\text{-}iso)]^{2+}$, 88496-36-0; $[(NH_3)_5Co(Gly\text{-}iso)]^{2+}$, 69421-30-3; $[(NH_3)_5Co(Pro\text{-}iso)]^{2+}$, 88496-37-1; $[(NH_3)_5Co(Phe\text{-}iso)]^{2+}$, 88496-38-2; $[(NH_3)_5Co(ProPro\text{-}iso)]^{2+}$, 88496-39-3; $[(NH_3)_5Co(GlyLeu\text{-}iso)]^{2+}$, 88496-40-6; $[(NH_3)_5Co(PhePhe\text{-}iso)]^{2+}$, 88496-41-7; isonicotinic acid trifluoromethanesulfonate, 88496-42-8.

Electron Transfer across Polypeptides. 3. Oligoproline Bridging Ligands

Stephan S. Isied* and Asbed Vassilian

Contribution from the Department of Chemistry, Rutgers, The State University of New Jersey, New Brunswick, New Jersey 08903. *Received June 30, 1983*

Abstract: A series of cobalt(III)-L-ruthenium(III) binuclear complexes (I-V), with a bridging oligoproline peptide derivatized

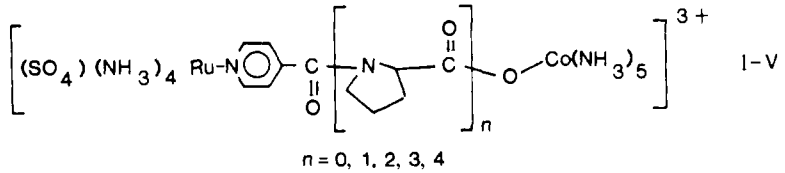

n = 0, 1, 2, 3, 4

with an isonicotinoyl (iso) group at the N-terminal, has been synthesized and purified by HPLC. These complexes provide a peptide spacer that separates the metal ions at distances determined by the peptide conformation and structure. Reduction of the above complexes to the precursor complex, the Co^{III}-L-Ru^{II} species, was followed by a slow rate of intramolecular electron transfer with unimolecular rate constants of 1.2×10^{-2}, 1.04×10^{-4}, 0.64×10^{-5}, 5.6×10^{-5}, and 1.4×10^{-4} s^{-1} for $n = 0$, 1, 2, 3, and 4. Over 2000 times variation in rate is seen for this series of binuclear complexes, which have identical reduction potentials, inner-sphere reorganization energies, and charge types. A decrease in rate by introducing $(Pro)_1$ and $(Pro)_2$ reflects an increase in the separation between the donor and acceptor. For the $(Pro)_3$ and $(Pro)_4$ compounds, the slow rate of electron transfer allows enough time for the conformation change of the proline to bring the two metal ions into close proximity, resulting in a more rapid rate of electron transfer.

The amino acid proline (**1**) occupies a unique position among the other naturally occurring amino acids (**2**). The cyclic structure of its side chain restricts rotation about the C-N bond within a proline residue and also about the peptide bond formed between

0002-7863/84/1506-1732$01.50/0